Journal of Applied Physics

AIP Publishing

Enhancing Ferroelectrics with Insulators: Band Offsets at the $Al_2O_3/BaTiO_3$ Interface

Shay Zimmerman[1], Yiying Xu[2,3], Maria Baskin[1], Yachin Ivry[2,3] and Lior Kornblum[1,a)]

[1] Technion Israel Institute of Technology, Haifa 32000-03, Israel; Andrew and Erna Viterbi Department of Electrical and Computer Engineering
[2] Technion Israel Institute of Technology, Haifa 32000-03, Israel; Solid State Institute
[3] Technion Israel Institute of Technology, Haifa 32000-03, Israel; Department of Materials Science and Engineering

Engineering ferroelectric interfaces is key to improving device performance. Combining thin insulators with ferroelectrics is a promising approach for minimizing leakage currents and increasing the switching efficiency. In this work we study the interface between atomic layer deposited amorphous Al_2O_3 and epitaxial $BaTiO_3$ films. These materials constitute simple and robust examples of an insulator and a ferroelectric, respectively. We confirm the microstructure and interface chemistry of the heterostructure. X-ray photoelectron spectroscopy was employed to quantify the interfacial bands offsets, yielding energy barriers of 1.3 eV for holes and 2.1 eV for electrons. These results highlight Al_2O_3 as a promising candidate for an insulating layer on ferroelectrics, paving the way for efficient insulator-ferroelectrics structures for ferroelectric functional devices.

[a)] Corresponding author: liork@technion.ac.il

I. INTRODUCTION

Ferroelectrics constitute some of the most studied and technologically-mature functional materials[1]. In microelectronics, ferroelectrics open new routes for fast and energy-efficient devices, such as the ferroelectric field effect transistor (FeFET), a candidate for improved subthreshold performance, and a promising technology for high-performance memory devices, with applications in logic-in-memory architectures, and neuromorphic, biology-inspired computing[2,3]. In photonics, ferroelectrics unlock efficient integrated light modulators with potential for additional active components[4–6]. In other fields ferroelectrics have shown attractive prospects in photovoltaics, catalysis, sensors and actuators[7–11].

A key component of the performance of functional ferroelectric devices is the ability to efficiently switch the ferroelectric layer. Two important aspects of this requirement are surface chemistry, and leakage currents through the ferroelectric. Surface chemistry can have significant influence on switching and on surface polarization[12]. Leakage currents can compromise the ability to apply an electric field over the ferroelectric layer, or result in damage caused by uncontrolled currents.

Surface and interface engineering of ferroelectrics is a promising approach to overcome the above challenges. The addition of an insulating layer on the surface of a ferroelectric can help obtaining chemically well-defined interfaces, while the insulator itself can reduce leakage currents. Furthermore, adding an insulating layer on top (or the bottom) of a ferroelectric is a useful approach for improving ferroelectric tunnel junctions (FTJ) performance, where the scheme is sometimes termed 'composite barrier'[13,14]. The interfacial band offsets are a crucial aspect of whether an interface can be insulating[15–17]. For example, by using a capping layer of Zr doped AlO_x , the ferroelectric polarization of

HfO_{2-x} was largely improved[18], and the insertion of Al_2O_3 layer into $Hf_{0.5}Zr_{0.5}O_2$ ferroelectrics heralded ultra-high energy storage performance[19].

In recent years increasing fundamental evidence point to the crucial importance of surface chemistry and defects in determining the functional properties and performance of ferroelectrics[20–22]. The incorporation of a surface insulating layer can change the surface chemistry in various manners, with potential effects on the ferroelectric functionality and device performance. We note that air exposure is another important facet of functional oxides[23,24]. The current work however, focuses on the effects of an ex-situ thin Al_2O_3 layer, and as such all the BTO surfaces in this work have been exposed to the air.

Here we examine the interface between the insulator Al_2O_3 and the ferroelectric $BaTiO_3$ (BTO). Al_2O_3 is a common, simple and robust insulator, and BTO is one of the most studied ferroelectrics, with particular interest in integrated photonics[25,26]. This material combination therefore combines simplicity, robustness and technological compatibility, making it a useful test case. Here we analyze the structure and interfacial chemistry and band offsets. We observe the expected surface chemistry with some non-stoichiometric Ba-rich interface phase. Importantly, we measure significant (>1 eV) band offsets at the interface, representing energy barriers for electrons and holes. These results indicate the potential of Al_2O_3 to preserve the surface chemistry of BTO and block leakage currents. Therefore, this Al_2O_3-BTO combination shows potential for improving the performance of various functional ferroelectric devices.

II. EXPERIMENTAL

8 nm of BTO were grown on TiO_2-terminated $SrTiO_3$ (STO) substrate (Crystal GmbH) using pulsed laser deposition (PLD) equipped with an excimer KrF laser (248nm). The laser energy and frequency were ~1.2 mJ/cm^{-2} and 2 Hz, resulting in a growth rate of 66 pulses per monolayer. Before deposition, the substrate was heated to 670 °C using a SiC heater at a rate of 5 °C/min at 100 mTorr of oxygen, where it was annealed for 15 min prior to BTO deposition. Following deposition, the sample was annealed at the deposition temperature and oxygen pressure for 30 min. The oxygen was pumped out after the sample was cooled to 300°C. 3 nm of amorphous Al_2O_3 (alumina) layer were deposited ex-situ onto the BTO surface by atomic layer deposition (ALD) at 300 °C using trimethyl-aluminum (TMA) and H_2O (the full details are reported in a previous work[15]). Atomic force microscopy (AFM, Asylum MFP-3D Infinity) was used in tapping mode for topography mapping. X-ray photoelectron spectroscopy (XPS, PHI Versaprobe III) spectra were acquired using a monochromatic Al Kα source (1486.6eV), and curve fitting was done using the CasaXPS software using 70:30% Gaussian/Lorentzian ratio after a Shirley-type background subtraction. Dual-beam neutralization was used to remove static charges at the surface. The binding energies were calibrated with reference to the Ti 2p 3/2 peak at 458.40 eV[11]. X-ray diffraction (XRD, Rigaku SmartLab 9 KW) was performed using a Cu Kα source (λ= 1.5406 Å) and a 2-bounce Ge monochromator, and curve fitting was done using GlobalFit 2.0 software.

III. RESULTS AND DISCUSSION

We start by characterizing the structure of the Al_2O_3/BTO bilayer, followed by its interfacial chemistry and then conclude with the band offsets. The surface topography of the Al_2O_3/BTO film measured by AFM (Figure 1) shows a step-terrace structure, with

atomically flat terraces and ~4 Å step height. These results indicate a high-quality growth of the BTO film as well as a smooth and uniform Al_2O_3 layer.

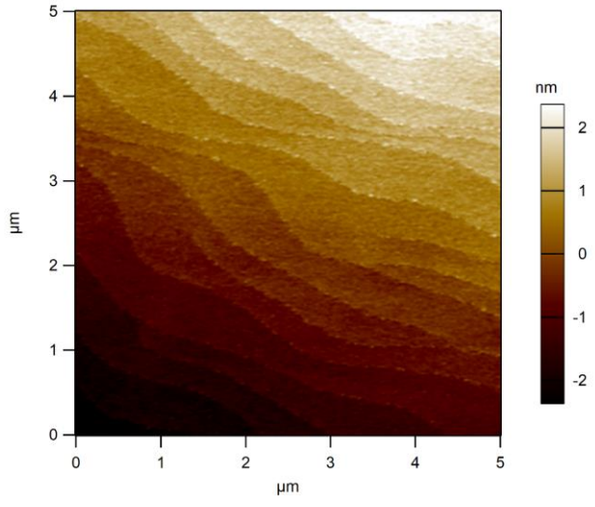

Figure 1: AFM image of the surface of 3 nm of Al_2O_3 on 8 nm of BTO

XRD analysis of the BTO film on an STO substrate is presented in Figure 2. The broad 2θ-ω scan (Figure 2a) shows the expected BTO and substrate (00L) reflections and no secondary phases, illustrating epitaxial growth of the BTO thin film on the (001)-oriented STO substrate. A feature at 38° could be the result of a miniscule amount of non-stoichiometric BTO[27,28], but its intensity is negligible compared to the film diffraction peaks. The ω scan of the (002) reflection (Figure 2b) exhibits a narrow FWHM of 0.17°, indicating high crystalline quality for such a thin film. Curve fitting for the out-of-plane lattice parameter yields out-of-plane lattice parameter values of 4.085 Å for the (001) peak and 4.095 Å is fitted for the (002) peak. These values are larger than the bulk of 3.994 Å (a-axis) and 4.038 Å (c-axis), suggesting that the BTO thin film is not fully strained. The lattice mismatch with the STO substrate is 2.2% for the c-oriented case, and 2.3% and 3.3% for the a-oriented case (in the two in-plane directions). In the

fully-strained BTO scenario, employing Poisson's ratio of 0.35,[29] the expected lattice parameters are 4.14Å (c-oriented) and 4.12Å (a-oriented), which are larger than the measured values, suggesting that the BTO is partially strained. It should be further noted that cation off-stoichiometry can cause the observed lattice parameter increase[30].

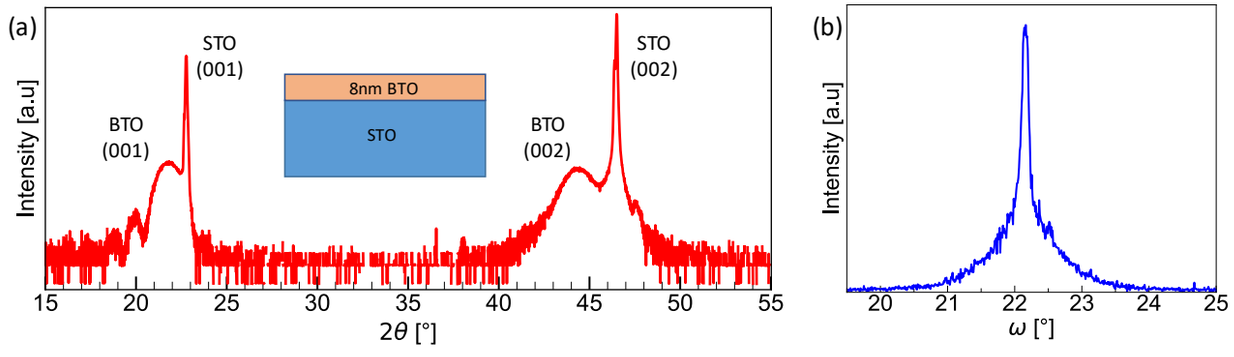

Figure 2: (a) XRD scan of the BTO/STO sample: θ/2θ,(b) ω scan of BTO/STO for the (002) peak of BTO. the inset shows a schematic drawing of the sample

XPS was acquired from the sample surface before and after deposition of 3 nm Al_2O_3. The Ti $2p_{3/2}$ XPS spectra of both the BTO/STO and the Al_2O_3/BTO surfaces (Figure 3a) correspond to Ti^{+4}, the nominal state of BTO [31] (Table I). No under-oxidized titanium (Ti^{+3}) is observed, within the detection limit that we estimate to be better than 2% at.[32,33]. We note that for transition metals the assignment of a single formal oxidation state is not always trivial, and our discussion of Ti in this context is over-simplified for clarity[34]. The excellent agreement between both spectra indicates that no observable redox reaction occurs during the ALD Al_2O_3 deposition process. The agreement between the Al 2p spectra of the thin (3 nm) Al_2O_3 on BTO and a thick (10 nm) Al_2O_3 from a previous work[15] (Figure 3b) validates the consistency of the properties of Al_2O_3 at ultrathin thickness.

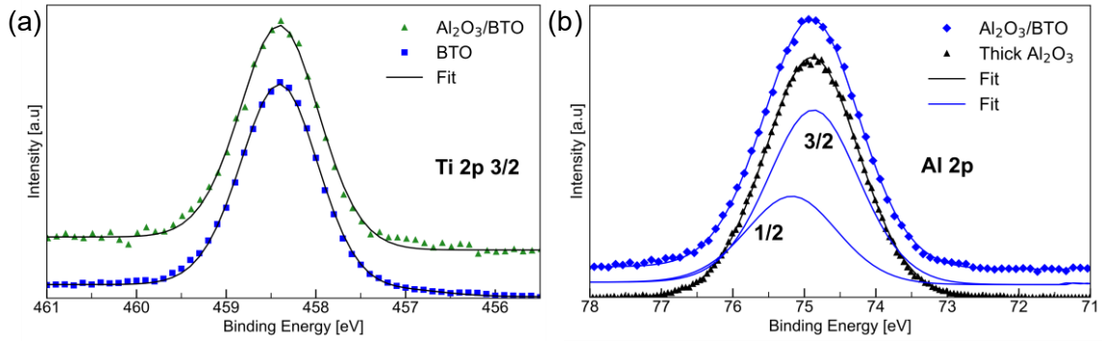

Figure 3: (a) XPS spectra of Ti $2p_{3/2}$ from the BTO surface, before and after ALD deposition of Al_2O_3. The binding energies are 458.40±0.05 eV. (b) XPS spectra of Al 2p from an ultrathin Al_2O_3 layer on top of a BTO, compared to a thicker Al_2O_3 from a previous work[15]. The binding energies of the 3/2 components are 74.52±0.05 eV and 74.77±0.05 eV, respectively. For comparison of the line shapes, the binding energy of thick Al_2O_3 was shifted by -0.25eV. The 2p 3/2 and 1/2 components of the fits are presented for Al_2O_3/BTO.

The Ba 3d doublets can each be fitted with two components. The spin-orbit value is 15.31eV in agreement with the literature[35]. The lower-binding-energy component (Ba I) corresponds to Ba from the bulk of the BTO (Table I). The higher-binding-energy component (Ba II) is commonly attributed to surface phases or contamination of the BTO surface which may originate by BaO_2[36,37], indicating surface Ba excess. In both cases the Ba oxidation state is +2. The Ba II percentage of the Al_2O_3/BTO sample was lower by ~5% versus the BTO sample. Altogether the chemical state of the Al_2O_3/BTO is found to be in agreement to expectations and the literature, with confirmed well-defined single oxidation states for Ti and Al. The absence of significant foreign diffraction peaks (Figure 2) and highly smooth surface (Figure 1) indicate that this secondary phase is likely amorphous and on the BTO surface.

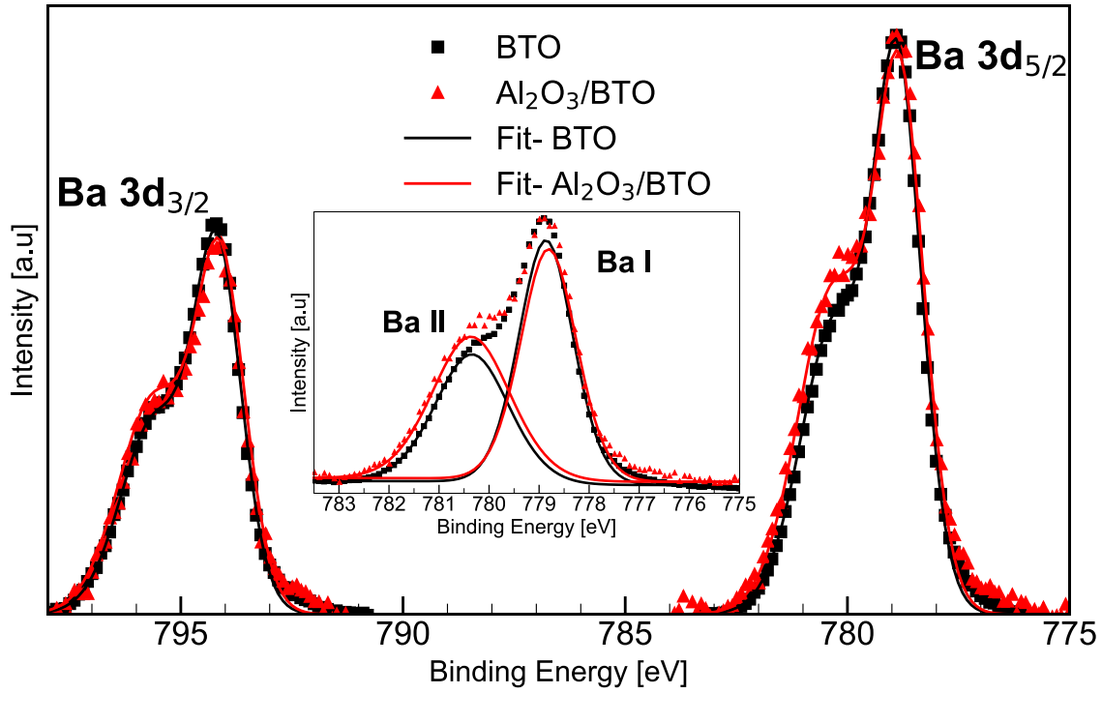

Figure 4: XPS spectra of Ba 3d of a BTO/STO and of Al_2O_3/BTO. The inset shows a magnified Ba $3d_{5/2}$ region with the fits of Ba I and Ba II components (see text for details).

Table I. The binding energy values of the core levels before and after Al_2O_3 deposition. The values have an uncertainty level of ±0.05 eV

Sample	Al 2p3/2 [eV]	Ti 3p [eV]	Ti 2p3/2 [eV]	Ba 3d 5/2 [eV]		Ba 3d 3/2 [eV]	
				Ba I	Ba II	Ba I	Ba II
bare BTO	-	36.28	458.40	778.86	780.34	794.17	795.65
Al_2O_3/BTO	74.52	36.37	458.40	778.81	780.36	794.10	795.65

Having ascertained the structure and interface chemistry of the Al_2O_3/BTO structure, we turn the focus to the interfacial band offsets. The valence band offset (VBO) at the Al_2O_3/BTO interface was determined using the Kraut method [38,39]

$$(1)\mathrm{VBO} = \mathrm{VBE}_{\mathrm{BTO}} - \mathrm{VBE}_{\mathrm{Al2O3}} = \mathrm{A} - \mathrm{B} - \mathrm{C}$$

$$(2)\ \mathrm{A} = \mathrm{BE}_{\mathrm{Ti\ 2p}}^{\mathrm{BTO}} - \mathrm{VBE}_{\mathrm{BTO}} = 455.9\mathrm{eV}$$

$$(3)\ \mathrm{B} = \mathrm{BE}_{\mathrm{Ti\ 2p}}^{\mathrm{Al2O3/BTO}} - \mathrm{BE}_{\mathrm{Al\ 2p\ 3/2}}^{\mathrm{Al2O3/BTO}} = 383.9\mathrm{eV}$$

$$(4)\ C = BE_{Al\,2p\,3/2}^{Al2O3} - VBE_{Al2O3} = 70.7eV$$

Where VBE_X is the valence band edge of material X (BTO or Al_2O_3), respectively, and BE_X^Y is the binding energy of the element X in material Y. The analysis yields a VBO of 1.3 ± 0.2 eV. Using the known values of the band gaps for BTO and Al_2O_3 the conduction band offset (CBO) was then calculated as:

$$(5)\ CBE_{Al2O3} - CBE_{BTO} = E_g^{Al2O3} - E_g^{BTO} - (VBE_{BTO} - VBE_{Al2O3})$$

Where CBE_X is the conduction band edge of material E_g^X is the band gap of material X. The band gap value of Al_2O_3 used in this work (6.6 eV) corresponds to Al_2O_3 grown under comparable conditions[15]. The resulting CBO is 2.1 ± 0.3 eV [37–39]. The calculation was repeated using the Ti 3p (instead of Ti 2p 3/2), and it yielded consistent results within the margin of error. These values indicate that Al_2O_3 is a suitable insulating layer on top of BTO from a band structure perspective. The band structure (Figure 6) illustrates the interfacial barrier for both electrons and holes. The band gap value used for BTO corresponds to its bulk form and may differ when considering a thin film[42].

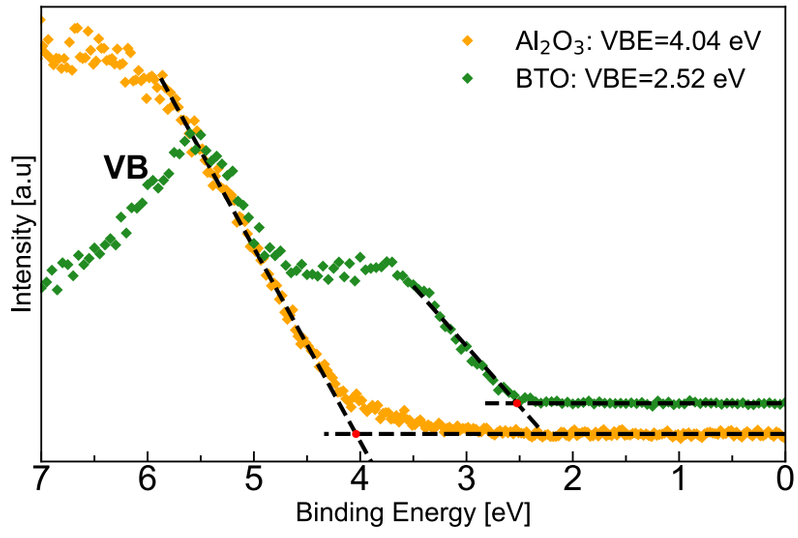

Figure 5: XPS spectrum of the valence band edges of the BTO and of Al_2O_3

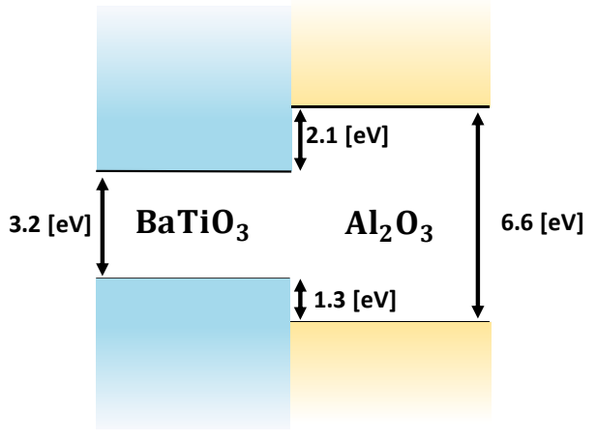

Figure 6: The band structure of BTO- Al_2O_3 interface

IV. SUMMARY AND CONCLUSIONS

The interface between Al_2O_3 and BTO was investigated using XPS. The analysis reveals that ex situ ALD growth of amorphous Al_2O_3 on BTO results in an insulating layer, with interfacial barriers of 1.3 eV for holes and 2.1 eV for electrons. The deposition process preserves the surface chemistry of BTO. These results suggest that Al_2O_3 is a promising insulating material for integration with ferroelectric BTO in electronic devices.

ACKNOWLEDGMENTS

The authors thank the Russell Berrie Nanotechnology Institute (RBNI) at the Technion for their generous seed (Nevet) funding support for this project. The authors further acknowledge support from the Technion's Micro-Nano Fabrication Unit (MNFU), Technion's Hellen Diller Quantum Center (HDQC) and the Grand Technion Energy Program (GTEP). In addition, we are grateful to Dr. Rajesh Mandel for fruitful discussions and to Dr. Kami Weinfeld for XPS measurements. YI acknowledges support from the Zuckerman STEM Leadership Program, and Israel Science Foundation (ISF) support under grant #3168/23. LK acknowledges support from ISF grant 1397/24.

AUTHOR DECLARATIONS

Conflicts of Interest

The authors have no conflicts to disclose.

REFERENCES

[1] L.W. Martin, and A.M. Rappe, "Thin-film ferroelectric materials and their applications," Nat. Rev. Mater. **2**(2), 16087 (2016).
[2] N. Zagni, F.M. Puglisi, P. Pavan, and M.A. Alam, "Reliability of HfO_2 -Based Ferroelectric FETs: A Critical Review of Current and Future Challenges," Proc. IEEE **111**(2), 158–184 (2023).
[3] S. Yu, "Neuro-Inspired Computing With Emerging Nonvolatile Memorys," Proc. IEEE **106**(2), 260–285 (2018).
[4] J. Geler-Kremer, F. Eltes, P. Stark, D. Stark, D. Caimi, H. Siegwart, B. Jan Offrein, J. Fompeyrine, and S. Abel, "A ferroelectric multilevel non-volatile photonic phase shifter," Nat. Photonics **16**(7), 491–497 (2022).
[5] Y. Wen, H. Chen, Z. Wu, W. Li, and Y. Zhang, "Fabrication and photonic applications of Si-integrated LiNbO3 and BaTiO3 ferroelectric thin films," APL Mater. **12**(2), 020601 (2024).

[6] A.A. Demkov, and A.B. Posadas, "Si-integrated ferroelectrics for photonics and optical computing," MRS Bull. **47**(5), 485–493 (2022).
[7] S.M. Young, and A.M. Rappe, "First Principles Calculation of the Shift Current Photovoltaic Effect in Ferroelectrics," Phys. Rev. Lett. **109**(11), 116601 (2012).
[8] I. Grinberg, D.V. West, M. Torres, G. Gou, D.M. Stein, L. Wu, G. Chen, E.M. Gallo, A.R. Akbashev, P.K. Davies, J.E. Spanier, and A.M. Rappe, "Perovskite oxides for visible-light-absorbing ferroelectric and photovoltaic materials," Nature **503**(7477), 509–512 (2013).
[9] A.M. Kolpak, I. Grinberg, and A.M. Rappe, "Polarization Effects on the Surface Chemistry of PbTiO 3 -Supported Pt Films," Phys. Rev. Lett. **98**(16), 166101 (2007).
[10] A. Kakekhani, and S. Ismail-Beigi, "Ferroelectric-Based Catalysis: Switchable Surface Chemistry," ACS Catal. **5**(8), 4537–4545 (2015).
[11] P. Abbasi, M.R. Barone, Ma. De La Paz Cruz-Jáuregui, D. Valdespino-Padilla, H. Paik, T. Kim, L. Kornblum, D.G. Schlom, T.A. Pascal, and D.P. Fenning, "Ferroelectric Modulation of Surface Electronic States in $BaTiO_3$ for Enhanced Hydrogen Evolution Activity," Nano Lett. **22**(10), 4276–4284 (2022).
[12] W.A. Saidi, J.M.P. Martirez, and A.M. Rappe, "Strong Reciprocal Interaction between Polarization and Surface Stoichiometry in Oxide Ferroelectrics," Nano Lett. **14**(11), 6711–6717 (2014).
[13] J. Hwang, Y. Goh, and S. Jeon, "Physics, Structures, and Applications of Fluorite-Structured Ferroelectric Tunnel Junctions," Small **20**(9), 2305271 (2024).
[14] Z. Wen, and D. Wu, "Ferroelectric Tunnel Junctions: Modulations on the Potential Barrier," Adv. Mater. **32**(27), 1904123 (2020).
[15] D. Cohen-Azarzar, M. Baskin, and L. Kornblum, "Band offsets at amorphous-crystalline Al2O3–SrTiO3 oxide interfaces," J. Appl. Phys. **123**(24), 245307 (2018).
[16] S.A. Chambers, Y. Liang, Z. Yu, R. Droopad, J. Ramdani, and K. Eisenbeiser, "Band discontinuities at epitaxial SrTiO3/Si(001) heterojunctions," Appl. Phys. Lett. **77**(11), 1662–1664 (2000).
[17] F. Amy, A.S. Wan, A. Kahn, F.J. Walker, and R.A. McKee, "Band offsets at heterojunctions between SrTiO3 and BaTiO3 and Si(100)," J. Appl. Phys. **96**(3), 1635–1639 (2004).
[18] H.-H. Chen, R.-Y. Liao, W.-C. Chou, H.-H. Hsu, C.-H. Cheng, and C.-C. Huang, "Ferroelectric Polarization Enhancement in Hafnium-Based Oxides Through Capping Layer Engineering," IEEE J. Electron Devices Soc. **10**, 947–952 (2022).
[19] J. Shin, D.H. Shin, H. Seo, K.D. Kim, S. Choi, T.K. Kim, H. Paik, H. Song, S. Byun, I.S. Lee, and C.S. Hwang, "Ultra-high energy storage performance of field-induced ferroelectric Al2O3-inserted Hf0.5Zr0.5O2 thin films for electrostatic supercapacitors," Energy Storage Mater. **79**, 104306 (2025).
[20] M. Barzilay, T. Qiu, A.M. Rappe, and Y. Ivry, "Epitaxial TiO_x Surface in Ferroelectric $BaTiO_3$: Native Structure and Dynamic Patterning at the Atomic Scale," Adv. Funct. Mater. **30**(18), 1902549 (2020).
[21] A. Hershkovitz, E. Hemaprabha, D. Khorshid, L. Ma, S. Liu, S. Cohen, and Y. Ivry, "Oxygen-vacancy mediated deterministic domain distribution at the onset of ferroelectricity," Acta Mater. **286**, 120738 (2025).

[22] J. Jeong, J. Hwang, Y. Xing, Z. Wang, J. Lee, and S.H. Oh, "Subsurface Oxygen Vacancy Mediated Surface Reconstruction and Depolarization of Ferroelectric $BaTiO_3$ (001) Surface," Adv. Sci., 2412781 (2025).
[23] S. Caspi, L. Shoham, M. Baskin, K. Weinfeld, C. Piamonteze, K.A. Stoerzinger, and L. Kornblum, "Effect of capping layers on the near-surface region of SrVO3 films," J. Vac. Sci. Technol. A **40**(1), 013208 (2022).
[24] A. Cohen, M. Baskin, L. Shoham, S. Caspi, P. Shekhter, T.-L. Lee, S.A. Chambers, and L. Kornblum, "Obtaining bulk-like correlated oxide surfaces with protective caps," Appl. Phys. Lett. **126**(16), 161602 (2025).
[25] F. Eltes, D. Caimi, F. Fallegger, M. Sousa, E. O'Connor, M.D. Rossell, B. Offrein, J. Fompeyrine, and S. Abel, "Low-Loss $BaTiO_3$ –Si Waveguides for Nonlinear Integrated Photonics," ACS Photonics **3**(9), 1698–1703 (2016).
[26] F. Eltes, C. Mai, D. Caimi, M. Kroh, Y. Popoff, G. Winzer, D. Petousi, S. Lischke, J.E. Ortmann, L. Czornomaz, L. Zimmermann, J. Fompeyrine, and S. Abel, "A $BaTiO_3$ - Based Electro-Optic Pockels Modulator Monolithically Integrated on an Advanced Silicon Photonics Platform," J. Light. Technol. **37**(5), 1456–1462 (2019).
[27]"ICDD card number 00-035-0817," (n.d.).
[28]"ICDD card number 00-035-0805," (n.d.).
[29] A.C. Dent, C.R. Bowen, R. Stevens, M.G. Cain, and M. Stewart, "Effective elastic properties for unpoled barium titanate," J. Eur. Ceram. Soc. **27**(13–15), 3739–3743 (2007).
[30] C.M. Brooks, L.F. Kourkoutis, T. Heeg, J. Schubert, D.A. Muller, and D.G. Schlom, "Growth of homoepitaxial SrTiO3 thin films by molecular-beam epitaxy," Appl. Phys. Lett. **94**(16), 162905 (2009).
[31] R.T. Haasch, E. Breckenfeld, and L.W. Martin, "Single Crystal Perovskites Analyzed Using X-ray Photoelectron Spectroscopy: 1. SrTiO3(001)," Surf. Sci. Spectra **21**(1), 87–94 (2014).
[32] M.S.J. Marshall, D.T. Newell, D.J. Payne, R.G. Egdell, and M.R. Castell, "Atomic and electronic surface structures of dopants in oxides: STM and XPS of Nb- and La-doped SrTiO 3 (001)," Phys. Rev. B **83**(3), 035410 (2011).
[33] D. Cohen-Azarzar, M. Baskin, A. Lindblad, F. Trier, and L. Kornblum, "Scalable and highly tunable conductive oxide interfaces," APL Mater. **11**(11), 111118 (2023).
[34] S.A. Chambers, P.V. Sushko, and P.S. Bagus, "Revisiting the assignment of atomic charges in metal oxides based on core-level x-ray photoelectron spectra: The case of Ti in SrTiO3(001)," J. Vac. Sci. Technol. A **43**(2), 023203 (2025).
[35] L.T. Hudson, R.L. Kurtz, S.W. Robey, D. Temple, and R.L. Stockbauer, "Surface core-level shifts of barium observed in photoemission of vacuum-fractured BaTiO 3 (100)," Phys. Rev. B **47**(16), 10832–10838 (1993).
[36] S. Chakrabarti, S. Ginnaram, S. Jana, Z.-Y. Wu, K. Singh, A. Roy, P. Kumar, S. Maikap, J.-T. Qiu, H.-M. Cheng, L.-N. Tsai, Y.-L. Chang, R. Mahapatra, and J.-R. Yang, "Negative voltage modulated multi-level resistive switching by using a Cr/BaTiOx/TiN structure and quantum conductance through evidence of H2O2 sensing mechanism," Sci. Rep. **7**(1), 4735 (2017).
[37] R. Contreras-Guerrero, J.P. Veazey, J. Levy, and R. Droopad, "Properties of epitaxial BaTiO3 deposited on GaAs," Appl. Phys. Lett. **102**(1), (2013).

[38] E.A. Kraut, R.W. Grant, J.R. Waldrop, and S.P. Kowalczyk, "Semiconductor core-level to valence-band maximum binding-energy differences: Precise determination by x-ray photoelectron spectroscopy," Phys. Rev. B **28**(4), 1965–1977 (1983).
[39] L. Kornblum, M.D. Morales-Acosta, E.N. Jin, C.H. Ahn, and F.J. Walker, "Transport at the Epitaxial Interface between Germanium and Functional Oxides," Adv. Mater. Interfaces **2**(18), 1500193 (2015).
[40] S. Balaz, Z. Zeng, and L.J. Brillson, "Heterojunction band offsets and dipole formation at BaTiO3/SrTiO3 interfaces," J. Appl. Phys. **114**(18), 183701 (2013).
[41] M. Cardona, "Optical Properties and Band Structure of SrTi O 3 and BaTi O 3," Phys. Rev. **140**(2A), A651–A655 (1965).
[42] S. Ramakanth, and K.C. James Raju, "Band gap narrowing in BaTiO3 nanoparticles facilitated by multiple mechanisms," J. Appl. Phys. **115**(17), (2014).